Hindawi Publishing Corporation
Mathematical Problems in Engineering
Volume 2013, Article ID 250683, 12 pages
http://dx.doi.org/10.1155/2013/250683

Research Article

Numerical Optimization Design of Dynamic Quantizer via Matrix Uncertainty Approach

Kenji Sawada and Seiichi Shin

Department of Mechanical Engineering and Intelligent Systems, The University of Electro-Communications, 1-5-1 Chofugaoka, Chofu, Tokyo, 182-8585, Japan

Correspondence should be addressed to Kenji Sawada; knj.sawada@uec.ac.jp

Received 12 July 2013; Accepted 12 September 2013

Academic Editor: Zidong Wang

In networked control systems, continuous-valued signals are compressed to discrete-valued signals via quantizers and then transmitted/received through communication channels. Such quantization often degrades the control performance; a quantizer must be designed that minimizes the output difference between before and after the quantizer is inserted. In terms of the broadbandization and the robustness of the networked control systems, we consider the continuous-time quantizer design problem. In particular, this paper describes a numerical optimization method for a continuous-time dynamic quantizer considering the switching speed. Using a matrix uncertainty approach of sampled-data control, we clarify that both the temporal and spatial resolution constraints can be considered in analysis and synthesis, simultaneously. Finally, for the slow switching, we compare the proposed and the existing methods through numerical examples. From the examples, a new insight is presented for the two-step design of the existing continuous-time optimal quantizer.

1. Introduction

With the rapid network technology development, the networked control systems (NCSs) have been widely studied [1–10]. One of the challenges in NCSs is quantized control. In NCSs, the continuous-valued signals are compressed and quantized to the discrete-valued signals via the quantizer of the communication channel, and such quantization often degrades the control performance. Hence, a desirable quantizer minimizes the performance error between before and after the quantizer insertion.

Motivated by this, researchers [11–14] have provided optimal dynamic quantizers for the following problem formulation in the discrete-time domain. For a given plant P, synthesize a "dynamic" quantizer Q_d such that the system Σ_Q composed of P and Q_d in Figure 1(a) "optimally" approximates the plant P in Figure 1(b) in the sense of the input-output relation. The obtained quantizer allows us to design various controllers for the plant P on the basis of the conventional control theories. Also, this framework is helpful in not only the NCS problem but also various control problems such as hybrid control, embedded system control, and on-off actuator control.

When we consider controlling a mechanical system with an on-off actuator, first the controlled object and its uncertainties are usually modeled in the continuous-time domain. Second, the model and its uncertainties are discretized to apply the above dynamic quantizer. However, the discretization sometimes results in uncertainties more complicated than those in the original model and creates undesirable complexity in robust control. The continuous-time setting quantizer is more suitable for the robust control of the quantized system than discrete-time one. Thus, our previous works [15, 16] have considered the continuous-time setting, while a number of the discrete-time settings have been studied by others [11–14]. In these works, it is assumed that the switching process of discretizing the continuous-valued signal is sufficiently quick relative to the control frequency and only the spatial determination (quantized accuracy) is considered as the quantization effect. This is

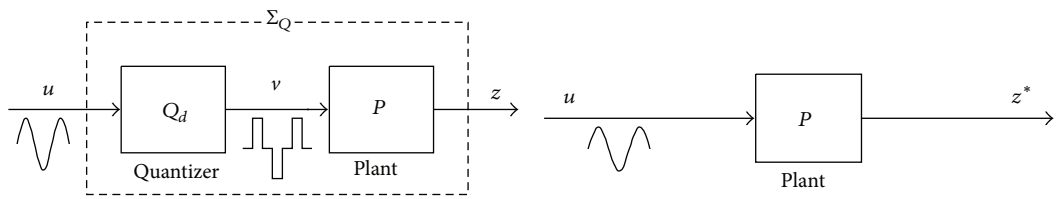

(a) Discrete-valued input system (b) Usual system

Figure 1: Two systems.

because the switching speed of the continuous-time delta-sigma modulator for wireless broadband network systems is from 1 MHz to 100 MHz [17, 18].

On the other hand, the above assumption is essentially weak in the case of the slow switching such as the mechanical systems with on-off actuators [19]. For the slow switching, we need to consider the quantization effect on both the switching speed and the spatial constraints in continuous time. For example, Ishikawa et al. proposed a two-step design of a feedback modulator [20]: (i) the control performance of the modulator is considered under only the spatial constraint, and (ii) the modulator is tuned in terms of the switching speed constraint. However, the structure of the modulator is more restricted than that of the dynamic quantizer and the obtained modulator is not always optimal. Therefore, the dynamic quantizer under temporal resolution (switching speed) and spatial resolution constraints has still to be optimally designed. The simultaneous consideration of the two constraints is the particular challenge we address in this paper.

We propose a numerical optimization method for the continuous-time dynamic quantizer under switching speed and quantized accuracy constraints. To achieve the method, this paper solves the design problem via sampled-data control framework that has so far provided various results for networked control problems [7–9]. We refer to the previous work on optimal dynamic quantizer design [11, 12] and consider the basic feedforward system in Figure 1(a). In addition to the invariant set analysis [21, 22] similarly to our previous works [13, 15, 16], this paper utilizes a matrix uncertainty approach [23, 24] that is proposed in a sampled-data control framework. Although the obtained results can be more conservative than those in the previous works on continuous-time dynamic quantizer [15, 16] from the viewpoint of the class of the exogenous input and the applicable plants, both temporal and spatial resolution constraints can be addressed in analysis and synthesis, simultaneously. For the fast switching case, the proposed conditions converge to the corresponding conditions of our previous works. Finally, for the slow switching, we compare the proposed and existing methods [15, 16] through numerical examples. In particular, a new insight is presented for the two-step design of the existing continuous-time optimal quantizer.

Notation. The set of $n \times m$ (positive) real matrices is denoted by $\mathbb{R}^{n\times m}$ ($\mathbb{R}_+^{n\times m}$). The set of $n \times m$ (positive) integer matrices is denoted by $\mathbb{N}^{n\times m}$ ($\mathbb{N}_+^{n\times m}$). We denote by $\mathscr{L}_\infty^p$ the set of piecewise-continuous functions of p-dimensional finite vectors such that ∞-norm of its functions is finite. $0_{n\times m}$ and I_m (or for simplicity of notation, 0 and I) denote the $n \times m$ zero matrix and the $m \times m$ identity matrix, respectively. For a matrix M, M^T, $\rho(M)$ and $\sigma_{\max}(M)$ denote its transpose, its spectrum radius, and its maximum singular value, respectively. For a vector x, x_i is the ith entry of x. For a symmetric matrix X, $X > 0$ ($X \geq 0$) means that X is positive (semi) definite. For a vector x and a sequence of vectors $X := \{x_1, x_2, \ldots\}$, $\|x\|$ and $\|X\|$ denote their ∞-norms, respectively. Finally, we use the "packed" notation $\left(\begin{array}{c|c} A & B \\ \hline C & D \end{array}\right) := C(sI - A)^{-1}B + D$.

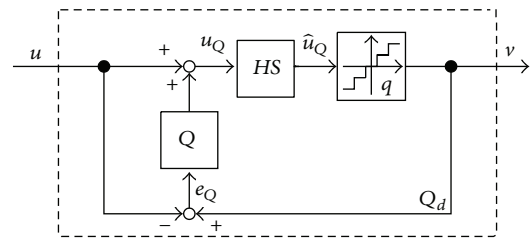

Figure 2: Continuous-time dynamic quantizer with switching speed h.

2. Problem Formulation

Consider the discrete-valued input system Σ_Q in Figure 1(a), which consists of the linear time invariant (LTI) continuous-time plant P and the quantizer $v = Q_d(u)$. The system P is given by

$$P : \begin{bmatrix} \dot{x} \\ z \end{bmatrix} = \begin{bmatrix} A & B \\ C & 0 \end{bmatrix} \begin{bmatrix} x \\ v \end{bmatrix}, \tag{1}$$

where $x \in \mathbb{R}^n$, $z \in \mathbb{R}^q$, $u \in \mathbb{R}^m$, and $v \in \mathbb{R}^m$ denote the state vector, the measured output, the exogenous input, and the quantizer output, respectively. The continuous-valued signal u is quantized into the discrete-valued signal v via the quantizer Q_d. We assume that the matrix A is Hurwitz; that is, the usual system in Figure 1(b) is stable in the continuous-time domain. The initial state is given as $x(0) = x_0$.

For the system P, consider the continuous-time dynamic quantizer $v = Q_d(u)$ with the state vector $x_Q \in \mathbb{R}^{n_Q}$ as shown in Figure 2. Its switching speed $h \in \mathbb{R}_+$ (or its temporal resolution) is determined by the operator HS, which converts

the continuous-time signal g into the low temporal resolution signal $\widehat{g}$ as follows:

$$\begin{aligned} HS : g \longrightarrow \widehat{g} : \widehat{g}(kh+\theta) = g[k], \\ g[k] = g(kh), \quad k = 0,1,2,3,\ldots, \ \theta \in [0,h). \end{aligned} \tag{2}$$

That is, $\widehat{u}_Q = HSu_Q$. S is the ideal sampler with the sampling period h and H is the zero-order hold operator. The spatial resolution of the quantizer Q_d is expressed by the static quantizer $q : \mathbb{R}^m \to d\mathbb{N}^m$ with the quantization interval $d \in \mathbb{R}_+$, that is,

$$v = q(HSu_Q), \qquad u_Q = u + v_Q \tag{3}$$

and the continuous-time LTI filter Q is given by

$$\begin{bmatrix} \dot{x}_Q \\ v_Q \end{bmatrix} = \begin{bmatrix} A_Q & B_Q \\ C_Q & 0 \end{bmatrix} \begin{bmatrix} x_Q \\ e_Q \end{bmatrix}, \qquad e_Q := v - u. \tag{4}$$

Note that q is of the nearest-neighbor type toward $-\infty$ such as the midtread quantizer in Figure 3 ($\|q_i(\widehat{u}_{Qi}) - \widehat{u}_{Qi}\| \le d/2$ where q_i and $\widehat{u}_{Qi}$ are the ith row of q and $\widehat{u}_Q$) and the initial state is given by $x_Q(0) = 0$ for the drift free of Q_d [11, 12].

Remark 1. In synthesis, our previous works [15, 16] ignored the operator HS. In implementation, however, the continuous-time quantizer needs the switching process discretizing the continuous-valued signal. Of course, the applicable interval of switching depends on controlled objects such as narrowband or broadband networked systems and mechanical systems with on-off actuators. Therefore, it is important to consider the operator HS in synthesis.

For the system Σ_Q in Figure 1(a) with the initial state x_0 and the exogenous input $u \in \mathscr{L}_\infty^m$, $z(t, x_0, Q_d(u))$ denotes the output of z at the time t. Also, for the system in Figure 1(b) without Q_d, $z^*(t, x_0, u)$ denotes its output at the time t. Consider the following cost function:

$$\begin{aligned} &J(Q_d) \\ &\quad := \sup_{(x_0,u)\in\mathbb{R}^n\times\mathscr{L}_\infty^m} \ \sup_{t\in\mathbb{R}_+\cup\{0\}} \left\| z(t, x_0, Q_d(u)) - z^*(t, x_0, u) \right\|. \end{aligned} \tag{5}$$

If the quantizer minimizes $J(Q_d)$, the system Σ_Q "optimally" approximates the usual system P in the sense of the input-output relation. In this case, we can use the existing continuous-time controller design methods for the system in Figure 1(b) without considering the quantization effect. When the controlled object and its uncertainties are modeled in the continuous-time domain, therefore, the continuous-time quantizer can introduce robust control of the continuous-time setting directly, while the discrete-time quantizer requires discretization of the whole control system. Our previous works [15, 16] proposed an optimal dynamic quantizer for the cost function $J(Q_d)$ for the fast switching case $h = 0$. That is, only the spatial deterioration has been considered.

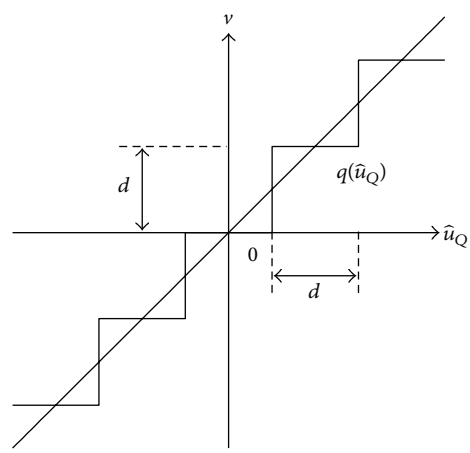

Figure 3: Midtread quantization.

On the other hand, the simultaneous consideration of the temporal and spatial resolution constraints is the problem we address in this paper. To consider the temporal resolution constraint caused by the operator HS, this paper modifies the cost function as follows:

$$\begin{aligned} &J_{HS}(Q_d) \\ &\quad := \sup_{(x_0,u)\in\mathbb{R}^n\times\mathscr{L}_\infty^m} \ \sup_{\theta\in[0,h)} \ \sup_{k\in\mathbb{N}_+\cup\{0\}} \left\| z(kh+\theta, x_0, Q_d(u)) \right. \\ &\qquad\qquad \left. - z^*(kh+\theta, x_0, u) \right\|. \end{aligned} \tag{6}$$

Fixing $\theta = 0$ ignores the output error between before and after the quantizer is inserted over the kth sampling interval and leads to the cost function setting that is utilized for the discrete-time optimal dynamic quantizers [11–14]. Therefore, the optimal quantizer for $J_{HS}(Q_d)$ minimizes the output error between the systems in Figures 1(a) and 1(b) in terms of the input-output relation under the temporal and spatial resolution constraints.

Motivated by the above, our objective is to solve the following continuous-time dynamic quantizer synthesis problem **(E)**: *for the system Σ_Q composed of P and Q_d with the initial state $x_0 \in \mathbb{R}^n$ and the exogenous input $u \in \ell_\infty^m$, suppose that the quantization interval $d \in \mathbb{R}_+$, the switching speed $h \in \mathbb{R}_+$, and the performance level $\gamma \in \mathbb{R}_+$ are given. Characterize a continuous-time dynamic quantizer Q_d* (i.e., *find parameters (n_Q, A_Q, B_Q, C_Q)) achieving $J_{HS}(Q_d) \le \gamma$.*

This paper proposes continuous-time quantizers in terms of solving the problem **(E)** on the basis of invariant set analysis and the sampled-data control technique, while other researchers [11, 12, 14] have proposed the discrete-time optimal ones.

Remark 2. The cost function setting of this paper is more complicated than the existing continuous-time and discrete-time cases [11–16], so this paper considers the basic feedforward system composed of P and Q_d similar to the previous works on optimal dynamic quantizer design [11, 12].

Remark 3. The plant P is restricted to be stable because of the feedforward structure, while the existing results can address unstable plants. To remove this restriction, we need to consider a feedback system structure similar to existing ones [13–16]. This is our future task.

3. Main Result

3.1. System Expression. In this subsection, we consider the system expression for the quantizer analysis. Define the quantization error e as

$$e := q(\widehat{u}_Q) - \widehat{u}_Q = v - \widehat{u}_Q. \tag{7}$$

From the properties of the quantizer q and the operator HS,

$$e(kh+\theta) = e[k] \in \left[-\frac{d}{2}, \frac{d}{2}\right]^m, \quad k = 0, 1, 2, \ldots, \ \theta \in [0, h), \tag{8}$$

holds where $e[k] = e(kh)$. Then, one obtains

$$v(kh+\theta) = v_Q[k] + u[k] + e[k], \tag{9}$$

where $v_Q[k] = v_Q(kh)$ and $u[k] = u(kh)$ for $k = 0, 1, 2, \ldots$, $\theta \in [0, h)$. In this case, by using the sampled-data control technique, the following lemma holds.

Lemma 4. *Denote by $\widehat{x}$ the state vector of the usual system in Figure 1(b) and define the signals as follows:*

$$\xi := \left[x^T - \widehat{x}^T \ \ x_Q^T\right]^T, \qquad z_p := z - z^*. \tag{10}$$

For the cost function $J_{HS}(Q_d)$, the difference between $z(kh+\theta, x_0, Q_d(u))$ and $z^*(kh+\theta, x_0, u)$ for $k = 0, 1, 2, \ldots$, $\theta \in [0, h)$ is given by the following system:

$$\Sigma : \begin{cases} \xi[k+1] = \mathscr{A}\xi[k] + \mathscr{B}e[k] \\ \qquad + \begin{bmatrix} \int_0^h e^{A(h-\tau)} B\widetilde{u}(kh+\tau)\,\mathrm{d}\tau \\ \int_0^h e^{A_Q(h-\tau)} B_Q\widetilde{u}(kh+\tau)\,\mathrm{d}\tau \end{bmatrix} \\ z_p(kh+\theta) = \mathscr{C}(\theta)\xi[k] + \mathscr{D}(\theta)e[k] \\ \qquad + C\int_0^\theta e^{A(h-\tau)} B\widetilde{u}(kh+\tau)\,\mathrm{d}\tau, \end{cases} \tag{11}$$

where $\xi[0] = 0$, $\widetilde{u}(kh+\tau) := u[k] - u(kh+\tau)$; the matrices $\mathscr{A}$, $\mathscr{B}$, $\mathscr{C}(\theta)$, and $\mathscr{D}(\theta)$ are defined as follows:

$$\begin{aligned} \mathscr{A} &:= \begin{bmatrix} e^{Ah} & \int_0^h e^{A\tau}\mathrm{d}\tau BC_Q \\ 0 & e^{A_Q h} + \int_0^h e^{A_Q\tau}\mathrm{d}\tau B_Q C_Q \end{bmatrix}, \\ \mathscr{B} &:= \begin{bmatrix} \int_0^h e^{A\tau}\mathrm{d}\tau B \\ \int_0^h e^{A_Q\tau}\mathrm{d}\tau B_Q \end{bmatrix}, \\ \mathscr{C}(\theta) &:= \left[Ce^{A\theta} \ \ C\int_0^\theta e^{A\tau}\mathrm{d}\tau BC_Q\right], \\ \mathscr{D}(\theta) &:= C\int_0^\theta e^{A\tau}\mathrm{d}\tau. \end{aligned} \tag{12}$$

Proof. See Appendix A. □

We focus on $\widetilde{u}(kh+\tau)$ of Σ. For the operator HS and the signal $u \in \mathscr{L}_\infty^m$,

$$\lim_{h\to 0} \|[(I - HS)u](t)\| \neq 0 \tag{13}$$

holds. This implies that we cannot ignore the temporal resolution constraint on the cost function $J_{HS}(Q_d)$ even if $h \to 0$. On the other hand, low-pass prefiltering rectifies this situation [25]. In fact, for the stable LTI system F,

$$\begin{gathered} \lim_{h\to 0} \|[(I - HS)Fu](t)\| = 0, \\ F := \left(\left(\begin{array}{c|c} A_F & B_F \\ \hline C_F & 0 \end{array}\right)\right) \end{gathered} \tag{14}$$

holds. For the evaluation of the cost function $J_{HS}(Q_d)$, then this paper utilizes

$$u = HSFr, \quad r \in \mathscr{L}_\infty^m \tag{15}$$

as the exogenous input. Note that $u \in \mathscr{L}_\infty^m$ if stable F is strictly proper and $r \in \mathscr{L}_\infty^m$. For the signal (15), $u[k] = u(kh+\theta)$ ($k = 0, 1, 2, \ldots$, $\theta \in [0, h)$) holds, so the terms of $\widetilde{u}(kh+\tau)$ in (11) are eliminated. Then, Σ is rewritten as

$$\Sigma_{HS} : \begin{cases} \xi[k+1] = \mathscr{A}\xi[k] + \mathscr{B}e[k], \\ z_p(kh+\theta) = \mathscr{C}(\theta)\xi[k] + \mathscr{D}(\theta)e[k]. \end{cases} \tag{16}$$

Also, this paper solves the following synthesis problem **(E′)**: *for the system Σ_Q composed of P and Q_d with the initial state $x_0 \in \mathbb{R}^n$ and the exogenous input $u \in \mathscr{L}_\infty^m$ in* (15), *suppose that the quantization interval $d \in \mathbb{R}_+$,* the *switching speed $h \in \mathbb{R}_+$, and the performance level $\gamma \in \mathbb{R}_+$ are given. Characterize a continuous-time dynamic quantizer Q_d* (i.e., *find parameters (n_Q, A_Q, B_Q, C_Q)) achieving $J_{HS}(Q_d) \leq \gamma$.*

3.2. Quantizer Analysis. The quantization error e of (16) is bounded as mentioned earlier. The reachable set and the invariant set characterize such a system with bounded input. Consider the LTI discrete-time system given by

$$\tilde{\xi}[k+1] = \mathscr{A}\tilde{\xi}[k] + \mathscr{B}w[k], \tag{17}$$

where $\tilde{\xi} \in \mathbb{R}^{n_\xi}$ and $w \in \mathbb{R}^m$ denote the state vector and disturbance input, respectively. We define the reachable set and the invariant set.

Definition 5. Define the reachable set of the system (17) to be a set $\mathbb{R}_\infty$ which satisfies

$$\mathbb{R}_\infty := \left\{ \tilde{\xi} \in \mathbb{R}^{n_\xi} \;\middle|\; \begin{array}{c} \exists k \in \mathbb{N}_+ \quad \exists w[\cdot] \in \mathbb{W}, \\ \tilde{\xi}[k] = \sum_{i=0}^{k-1} \mathscr{A}^{k-1-i}\mathscr{B}w[i] \end{array} \right\},$$
$$\mathbb{W} := \left\{ w \in \mathbb{R}^m : w^T w \le 1 \right\}. \tag{18}$$

Definition 6. Define the invariant set of the system (17) to be a set x which satisfies

$$\tilde{\xi} \in x, \quad w \in \mathbb{W} \Longrightarrow \mathscr{A}\tilde{\xi} + \mathscr{B}w \in x. \tag{19}$$

The analysis condition can be expressed in terms of matrix inequalities as summarized in the following proposition [22].

Proposition 7. *Consider the system* (17). *For a matrix* $0 < \mathscr{P} = \mathscr{P}^T \in \mathbb{R}^{n_\xi \times n_\xi}$, *the ellipsoid* $\mathbb{E}(\mathscr{P}) := \{\tilde{\xi} \in \mathbb{R}^{n_\xi} : \tilde{\xi}^T\mathscr{P}\tilde{\xi} \le 1\}$ *is an invariant set if and only if there exists a scalar* $\alpha \in [0, 1-\rho(\mathscr{A})^2]$ *satisfying*

$$\begin{bmatrix} \mathscr{A}^T\mathscr{P}\mathscr{A} - (1-\alpha)\mathscr{P} & \mathscr{A}^T\mathscr{P}\mathscr{B} \\ \mathscr{B}^T\mathscr{P}\mathscr{A} & \mathscr{B}^T\mathscr{P}\mathscr{B} - \alpha I_m \end{bmatrix} \le 0. \tag{20}$$

Note that the ellipsoidal set $\mathbb{E}(\mathscr{P})$ covers the reachable set $\mathbb{R}_\infty$ from outside. Define the set $\mathscr{E} := \{\tilde{w} \in \mathbb{R}^m : e = (\sqrt{m}d/2)\tilde{w}$ satisfies (7)$\}$ and rewrite the system (16) as

$$\tilde{\Sigma}_{HS} : \begin{cases} \tilde{\xi}[k+1] = \boldsymbol{\mathscr{A}}\tilde{\xi}[k] + \boldsymbol{\mathscr{B}}\tilde{w}[k], \\ \tilde{z}_p(kh+\theta) = \boldsymbol{\mathscr{C}}(\theta)\tilde{\xi}[k] + \boldsymbol{\mathscr{D}}(\theta)\tilde{w}[k], \end{cases} \tag{21}$$

where $\xi = (\sqrt{m}d/2)\tilde{\xi}$, $z_p = (\sqrt{m}d/2)\tilde{z}_p$, $e = (\sqrt{m}d/2)\tilde{w}$, and $\tilde{w} \in \mathscr{E}$. The left multiplication of $\tilde{\Sigma}_{HS}$ with $\sqrt{m}d/2$ leads to Σ_{HS}. The relation $\mathscr{E} \subseteq \mathbb{W}$ clearly holds because $e^Te \le md^2/4$ and the set $\mathbb{W}$ is an independent bounded disturbance without the relation (7). That is, the reachable set of $\tilde{\Sigma}_{HS}$ with $\tilde{w} \in \mathscr{E}$ is no larger than that of $\tilde{\Sigma}_{HS}$ with the disturbance $\tilde{w} \in \mathbb{W}$.

Then, this paper utilizes the reachable set to estimate the influences of the quantization error and the invariant set to characterize the cost function $J_{HS}(Q_d)$ by substituting $\mathscr{A} = \boldsymbol{\mathscr{A}}$ and $\mathscr{B} = \boldsymbol{\mathscr{B}}$ into (20). Move on to the matrix exponential $e^{A\theta}$ of $\boldsymbol{\mathscr{C}}(\theta)$ and $\boldsymbol{\mathscr{D}}(\theta)$ in (21), which is rewritten as

$$e^{A\theta} = I + \Omega(\theta)A, \qquad \Omega(\theta) := \int_0^\theta e^{A\tau}\mathrm{d}\tau. \tag{22}$$

Along with this, $\tilde{z}_p$ of (21) is also rewritten as

$$\begin{aligned} &\tilde{z}_p(kh+\theta) \\ &\quad = \left[C + C\Omega(\theta)A \quad C\Omega(\theta)BC_Q\right]\tilde{\xi}[k] + C\Omega(\theta)\tilde{w}[k] \\ &\quad = \left(\widehat{\boldsymbol{\mathscr{C}}} + C\Omega(\theta)\widehat{\boldsymbol{\mathscr{D}}}\right)\tilde{\xi}[k] + C\Omega(\theta)\tilde{w}[k], \\ &\qquad \widehat{\boldsymbol{\mathscr{C}}} := \left[C \quad 0\right], \qquad \widehat{\boldsymbol{\mathscr{D}}} := \left[A \quad BC_Q\right]. \end{aligned} \tag{23}$$

In addition, from the properties of $\mathbb{R}_\infty$ and $\mathbb{E}(\mathscr{P})$,

$$\begin{aligned} &J_{HS}(Q_d) \\ &\le \sup_{\theta\in[0,h)} \sup_{\tilde{\xi}\in\mathbb{R}_\infty, \tilde{w}\in\mathscr{E}} \left\|\boldsymbol{\mathscr{C}}(\theta)\tilde{\xi} + \boldsymbol{\mathscr{D}}(\theta)\tilde{w}\right\| \frac{\sqrt{m}d}{2} \\ &\le \sup_{\theta\in[0,h)} \sup_{\tilde{\xi}\in\mathbb{R}_\infty, \tilde{w}\in\mathbb{W}} \left\|\boldsymbol{\mathscr{C}}(\theta)\tilde{\xi} + \boldsymbol{\mathscr{D}}(\theta)\tilde{w}\right\| \frac{\sqrt{m}d}{2} \quad (\because \mathscr{E} \subseteq \mathbb{W}) \\ &\le \sup_{\theta\in[0,h)} \sup_{\tilde{\xi}\in\mathbb{E}(\mathscr{P}), \tilde{w}\in\mathbb{W}} \left\|\boldsymbol{\mathscr{C}}(\theta)\tilde{\xi} + \boldsymbol{\mathscr{D}}(\theta)\tilde{w}\right\| \frac{\sqrt{m}d}{2} \\ &\qquad\qquad (\because \mathbb{R}_\infty \subseteq \mathbb{E}(\mathscr{P})) \\ &\le \underbrace{\sup_{\theta\in[0,h)} \sup_{\tilde{\xi}\in\mathbb{E}(\mathscr{P})} \left\|(\widehat{\boldsymbol{\mathscr{C}}} + C\Omega(\theta)\widehat{\boldsymbol{\mathscr{D}}})\tilde{\xi}\right\|}_{\gamma_1} \frac{\sqrt{m}d}{2} \\ &\quad + \underbrace{\sup_{\theta\in[0,h)} \sup_{\tilde{w}\in\mathbb{W}} \left\|C\Omega(\theta)\tilde{w}\right\|}_{\gamma_2} \frac{\sqrt{m}d}{2} \end{aligned} \tag{24}$$

holds. Similarly to our previous papers [13, 15, 16], by using the $\mathscr{L}_1$ control technique in [21], we provide the sufficient conditions for computing $\gamma_1 \in \mathbb{R}_+$ and $\gamma_2 \in \mathbb{R}_+$ of (24) as follows:

$$\begin{aligned} &\begin{bmatrix} \mathscr{P} & \widehat{\boldsymbol{\mathscr{C}}}^T + \widehat{\boldsymbol{\mathscr{D}}}^T\Omega(\theta)^TC^T \\ \widehat{\boldsymbol{\mathscr{C}}} + C\Omega(\theta)\widehat{\boldsymbol{\mathscr{D}}} & \gamma_1^2 I_q \end{bmatrix} \ge 0, \\ &\Omega(\theta)^TC^TC\Omega(\theta) \le \gamma_2^2 I_n, \quad \forall\theta \in [0,h). \end{aligned} \tag{25}$$

Remark 8. For the inequalities (25) and any vectors $\tilde{\xi} \in \mathbb{R}^n$ and $\tilde{w} \in \mathbb{R}^m$, we have

$$\begin{aligned} &\begin{bmatrix} \tilde{\xi}^T\mathscr{P}\tilde{\xi} & \tilde{\xi}^T\left(\widehat{\boldsymbol{\mathscr{C}}}^T + \widehat{\boldsymbol{\mathscr{D}}}^T\Omega(\theta)^TC^T\right) \\ \left(\widehat{\boldsymbol{\mathscr{C}}} + C\Omega(\theta)\widehat{\boldsymbol{\mathscr{D}}}\right)\tilde{\xi} & \gamma_1^2 I_q \end{bmatrix} \ge 0 \\ &\Longleftrightarrow \tilde{\xi}^T\left(\widehat{\boldsymbol{\mathscr{C}}} + C\Omega(\theta)\widehat{\boldsymbol{\mathscr{D}}}\right)^T\left(\widehat{\boldsymbol{\mathscr{C}}} + C\Omega(\theta)\widehat{\boldsymbol{\mathscr{D}}}\right)\tilde{\xi} \\ &\le \gamma_1^2\tilde{\xi}^T\mathscr{P}\tilde{\xi} \quad (\because \text{Schur complement}) \end{aligned} \tag{26}$$

and $\tilde{w}^T\Omega(\theta)^TC^TC\Omega(\theta)\tilde{w} \le \gamma_2^2\tilde{w}^T\tilde{w}$. Then, we see that (24) holds if $\tilde{\xi} \in \mathbb{E}(\mathscr{P})$ and $\tilde{w} \in \mathbb{W}$.

The inequalities (25) are difficult to test since we need to find $\mathscr{P}$, γ_1, and γ_2 satisfying (20) and (25) for infinitely many values of $\theta \in [0, h)$. Then, using the matrix uncertainty technique [23, 24], we consider their sufficient conditions, which are easy to compute. Considering $\Omega(\theta)$ in (22) as a matrix uncertainty, we introduce the following lemma regarding the matrix exponential [26, 27].

Lemma 9. *For the matrix $\Omega(\theta)$ in (22),*

$$\sigma_{\max}(\Omega(\theta)) \le \delta(\theta) \le \delta(h), \quad \forall \theta \in [0, h), \tag{27}$$

holds where

$$\delta(\theta) := \begin{cases} \dfrac{e^{\mu(A)\theta} - 1}{\mu(A)}, & \mu(A) \neq 0, \\ \theta, & \mu(A) = 0, \end{cases}$$
$$\mu(A) := \max\left\{\lambda : \lambda \in eig\left(\frac{\left(A + A^T\right)}{2}\right)\right\}. \tag{28}$$

Proof. Since $\sigma_{\max}(e^{A\theta}) \le e^{\mu(A)\theta}$ (see [26]),

$$\sigma_{\max}(\Omega(\theta)) \le \int_0^\theta \sigma_{\max}\left(e^{A\beta}\right) d\beta \le \int_0^\theta e^{\mu(A)\beta} d\beta \tag{29}$$

holds. □

By using Lemma 9 and the S-procedure [23, 28, 29], the sufficient condition analyzing the cost function $J_{HS}(Q_d)$ of the system Σ_Q can be expressed in terms of matrix inequality as summarized in the following theorem.

Theorem 10. *Consider the system Σ_Q composed of P and Q_d with the initial state $x_0 \in \mathbb{R}^n$ and the exogenous input $u \in \mathscr{L}_\infty^m$ in (15). For the quantization interval $d \in \mathbb{R}_+$ and the switching speed $h \in \mathbb{R}_+$, the upper bound of the cost function $J_{HS}(Q_d)$ is given by*

$$J_{HS}(Q_d) \le \gamma(h)$$
$$s.t.\ \gamma(h) := \left(\gamma + \sigma_{\max}(C)\,\delta(h)\right)\frac{\sqrt{m}d}{2} \tag{30}$$

if there exist $0 < \mathcal{Q} = \mathcal{Q}^T \in \mathbb{R}^{(n+n_Q)\times(n+n_Q)}$, $0 < S = S^T \in \mathbb{R}^{n\times n}$, $\alpha_h \in [0, 1/2h - \rho(\mathcal{A})^2/2h]$ and $\gamma \in \mathbb{R}_+$ satisfying

$$\begin{bmatrix} \Phi_h\mathcal{Q} + \mathcal{Q}\Phi_h^T + 2\alpha_h\mathcal{Q} & \Gamma_h & \sqrt{h}\mathcal{Q}\Phi_h^T \\ \Gamma_h^T & -2\alpha_h I_m & \sqrt{h}\Gamma_h^T \\ \sqrt{h}\Phi_h\mathcal{Q} & \sqrt{h}\Gamma_h & -\mathcal{Q} \end{bmatrix} \le 0, \tag{31}$$

$$\begin{bmatrix} \mathcal{Q} & \mathcal{Q}\widehat{\mathcal{C}}^T & \sqrt{\delta(h)}\mathcal{Q}\widehat{\mathcal{D}}^T \\ \widehat{\mathcal{C}}\mathcal{Q} & \gamma^2 I_q - \delta(h)CSC^T & 0 \\ \sqrt{\delta(h)}\widehat{\mathcal{D}}\mathcal{Q} & 0 & S \end{bmatrix} \ge 0, \tag{32}$$
$$S\Omega(\theta) = \Omega(\theta)S, \quad \forall \theta \in [0, h),$$

where the matrices Φ_h and Γ_h are defined by

$$\Phi_h := \begin{bmatrix} \dfrac{1}{h}\displaystyle\int_0^h e^{A\tau}d\tau A & \dfrac{1}{h}\displaystyle\int_0^h e^{A\tau}d\tau BC_Q \\ 0 & \dfrac{1}{h}\displaystyle\int_0^h e^{A_Q\tau}d\tau\left(A_Q + B_QC_Q\right) \end{bmatrix},$$
$$\Gamma_h := \begin{bmatrix} \dfrac{1}{h}\displaystyle\int_0^h e^{A\tau}d\tau B \\ \dfrac{1}{h}\displaystyle\int_0^h e^{A_Q\tau}d\tau B_Q \end{bmatrix}. \tag{33}$$

Proof. See Appendix A. □

Denote by $\widehat{\Sigma}$ the system Σ without operator HS. In this case, the system $\widehat{\Sigma}$ is given by

$$\widehat{\Sigma} : \dot{\xi}(t) = \widehat{\mathcal{A}}\xi(t) + \widehat{\mathcal{B}}e(t), \qquad z_p(t) = \widehat{\mathcal{C}}\xi(t), \tag{34}$$

where

$$\widehat{\mathcal{A}} := \begin{bmatrix} A & BC_Q \\ 0 & A_Q + B_QC_Q \end{bmatrix}, \qquad \widehat{\mathcal{B}} := \begin{bmatrix} B \\ B_Q \end{bmatrix}. \tag{35}$$

Regarding the definition of $\xi(t)$, see Lemma 4. An advantage the condition (31) over conditions (20) is that it can be used for a small h without numerical difficulty. This idea comes from [23, 24]. In the limit of $h \to 0$, $(1/h)\int_0^h e^{Ah}d\tau \to I$ and $(1/h)\int_0^h e^{A_Qh}d\tau \to I$ hold, so $\Phi_h \to \widehat{\mathcal{A}}$ and $\Gamma_h \to \widehat{\mathcal{B}}$ hold. In the same limit, from $\delta(h) \to 0$, conditions (31) and (32) converge to the analysis conditions of the continuous-time dynamic quantizer for the system $\widehat{\Sigma}$ in [15, 16]. On the other hand, for a small h, $e^{Ah} \to I$, $e^{A_Qh} \to I$, $\int_0^h e^{Ah}d\tau \to 0$ and $\int_0^h e^{A_Qh}d\tau \to 0$ hold, so $\mathcal{A}$ and $\mathcal{B}$ ($\mathcal{A}$ and $\mathcal{B}$) are close to identity and zero matrices, respectively, and the left side of (20) is close to zero.

In numerical computation, it is appropriate to fix the structure of S such that $S\Omega(\theta) = \Omega(\theta)S$ holds. For example, we can set $S = s_\theta I_n$, $s_\theta \in \mathbb{R}_+$ and this setting leads to the following optimization problem **(Aop)**:

$$\min_{\mathcal{Q}=\mathcal{Q}^T>0, S=s_\theta I_n>0, 1/2h-\rho(\mathcal{A})^2/2h\ge\alpha_h\ge0, \gamma>0} \gamma^2$$
$$\text{s.t. (31) and (32)}. \tag{36}$$

When scalar α_h is fixed, the conditions in Theorem 10 are linear matrix inequalities (LMIs) in terms of the other variables. Using standard LMI software and the line search of α_h, we can obtain an upper bound of $J_{HS}(Q_d)$.

3.3. Quantizer Synthesis. The problem **(Aop)** suggests that the quantizer synthesis problem $(\mathbf{E}')$ is reduced to the following nonconvex optimization problem **(OP)**:

$$\min_{\mathcal{Q}=\mathcal{Q}^T>0, S=s_\theta I_n>0, A_Q, B_Q, C_Q, 1/2h-\rho(\mathcal{A})^2/2h\ge\alpha_h\ge0, \gamma>0} \gamma^2$$
$$\text{s.t. (31) and (32)}. \tag{37}$$

That is, if **(OP)** is feasible, $(\mathbf{E}')$ is feasible.

From the matrix product such as $(1/h)\int_0^h e^{A_Q h}d\tau$ and $A_Q+B_QC_Q$ in (31), the synthesis condition is difficult to derive from Theorem 10 unlike the continuous-time case without the operator HS in [15, 16]. Thus, we fixed the parameters as follows:

$$n_Q = n, \qquad A_Q = A, \qquad B_Q = B. \tag{38}$$

The structure (38) does not severely limit the synthesis because A_Q and B_Q of the continuous-time dynamic quantizer for the system $\widehat{\Sigma}$ in [15, 16] are also (38). See Appendix B. In other words, $\dot{x}_Q = Ax_Q + Be_Q$ estimates the quantization influence on the system P. Along with this, we fix $\mathcal{Q}$ of (31) as follows:

$$\mathcal{Q} = \begin{bmatrix} Y & V \\ V & V \end{bmatrix}, \quad Y = Y^T > 0, \quad V = V^T > 0. \tag{39}$$

The structure (39) also does not impose a severe limitation on the synthesis because an appropriate choice of the quantizer state coordinates allows us to assume that $\mathcal{Q}$ has the special structure for the full order case $n_Q = n$ [30].

Under some circumstances (38) and (39), we obtain the following synthesis condition.

Theorem 11. *Consider the system Σ_Q composed of P and Q_d with the initial state $x_0 \in \mathbb{R}^n$ and the exogenous input $u \in \mathcal{L}_\infty^m$ in (15). Suppose that the quantization interval $d \in \mathbb{R}_+$, the switching speed $h \in \mathbb{R}_+$, and the performance level $\gamma \in \mathbb{R}_+$ are given. For a scalar $\alpha_h \in [0, 1/2h]$, there exist a continuous-time dynamic quantizer Q_d achieving (30) if one of the following equivalent statements holds.*

(i) *There exist matrices $0 < \mathcal{Q} = \mathcal{Q}^T \in \mathbb{R}^{(n+n_Q)\times(n+n_Q)}$, $0 < S = S^T \in \mathbb{R}^{n\times n}$ and a dynamic quantizer Q_d satisfying (31), (32), and (38).*

(ii) *There exist matrices $0 < Y = Y^T \in \mathbb{R}^{n\times n}$, $0 < V = V^T \in \mathbb{R}^{n\times n}$, $W \in \mathbb{R}^{m\times n}$, $0 < S = S^T \in \mathbb{R}^{n\times n}$ satisfying*

$$\begin{bmatrix} \Theta_{Ah} + \Theta_{Ah}^T + 2\alpha_h\Theta_P & \Theta_{Bh} & \sqrt{h}\Theta_{Ah}^T \\ \Theta_{Bh}^T & -2\alpha_h I_m & \sqrt{h}\Theta_{Bh}^T \\ \sqrt{h}\Theta_{Ah} & \sqrt{h}\Theta_{Bh} & -\Theta_P \end{bmatrix} \le 0, \tag{40}$$

$$\begin{bmatrix} \Theta_P & \Theta_C^T & \Theta_{Dh}^T \\ \Theta_C & \gamma^2 I_q - \delta(h)CSC^T & 0 \\ \Theta_{Dh} & 0 & S \end{bmatrix} \ge 0, \tag{41}$$

$$S\Omega(\theta) = \Omega(\theta)S, \quad \forall\theta \in [0, h),$$

where

$$\begin{aligned} \Theta_P &:= \begin{bmatrix} Y & V \\ V & V \end{bmatrix}, \qquad \Psi_h := \frac{1}{h}\int_0^h e^{A\tau}d\tau, \\ \Theta_{Ah} &:= \begin{bmatrix} \Psi_h(AY+BW) & \Psi_h(AV+BW) \\ \Psi_h(AV+BW) & \Psi_h(AV+BW) \end{bmatrix}, \\ \Theta_{Bh} &:= \begin{bmatrix} \Psi_h B \\ \Psi_h B \end{bmatrix}, \qquad \Theta_C := [CY \;\; CV], \\ \Theta_{Dh} &:= \left[\sqrt{\delta(h)}(AY+BW) \;\; \sqrt{\delta(h)}(AV+BW)\right]. \end{aligned} \tag{42}$$

In this case, such a quantizer parameter is given by

$$n_Q = n, \qquad A_Q = A, \qquad B_Q = B, \qquad C_Q = WY^{-1}. \tag{43}$$

Proof. We fix $\mathcal{Q}$ as shown in (39) and introduce the change of variables $W = C_QY$. Hence, (31) and (32) result in (40) and (41). Also, designing C_Q yields $\alpha_h \in [0, 1/2h]$ because $\rho(\mathcal{A})$ is determined by C_Q and $[0, 1/2h - \rho(\mathcal{A})^2/2h] \subseteq [0, 1/2h]$. □

In the limit of $h \to 0$; Ψ_h converges to I and $\delta(h)$ converges to 0; then conditions (40) and (41) also converge to the synthesis condition of the continuous-time dynamic quantizer for the system $\widehat{\Sigma}$ in (34). Also, by setting $S = s_\theta I_n$ for Theorem 11, the quantizer synthesis problem **(E′)** is reduced to the following optimization problem **(Sop)**:

$$\begin{aligned} &\min_{Y=Y>0^T, V=V^T>0, S=s_\theta I_n>0, W, 1/2h\ge\alpha_h\ge0, \gamma>0} \gamma^2 \\ &\text{s.t. } (40) \text{ and } (41). \end{aligned} \tag{44}$$

If **(Sop)** is feasible, **(E′)** is feasible. Therefore, a continuous-time dynamic quantizer considering both spatial and temporal resolution constraints is obtained from Theorem 11.

Remark 12. To consider numerical optimization analysis or synthesis of a quantizer as shown in **(Aop)** and **(Sop)**, we need the signal assumption (15) in Theorems 10 and 11. On the other hand, for the high speed switching such that h is very small, the assumption (15) ensures that solutions to the problem **(E′)** converge to our previous results [15, 16]. Therefore, the results of this paper partly include our previous results [15, 16] although each class of exogenous signals and plants is restricted.

4. Discussion

For the slow switching, we compare the proposed method and existing continuous-time quantizer [15, 16]. Consider the system Σ_Q. The plant P is the stable minimum phase LTI system:

$$\begin{bmatrix} \dot{x}(t) \\ z(t) \end{bmatrix} = \begin{bmatrix} -3 & 3 & 0 \\ 0 & -2 & 2 \\ 1 & 1 & 0 \end{bmatrix} \begin{bmatrix} x(t) \\ v(t) \end{bmatrix}. \tag{45}$$

In the case without the operator HS, an optimal form of the continuous-time quantizer Q_d^{op} [15, 16] is given by (B.2).

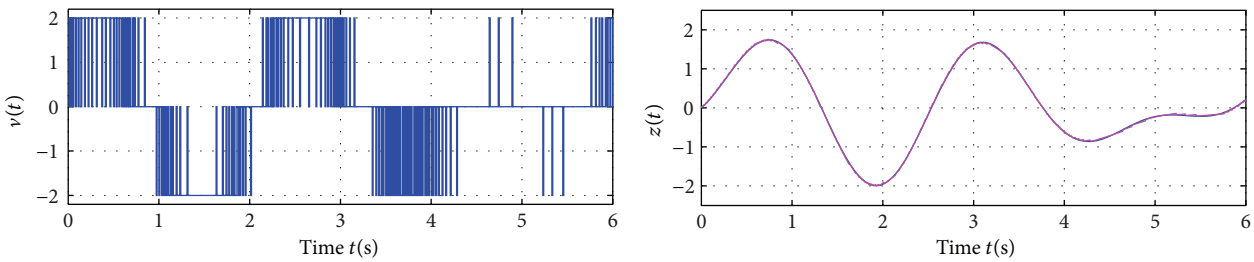

(a) (b)

FIGURE 4: Time responses of Σ_Q with the proposed quantizer for $h = 0.01$.

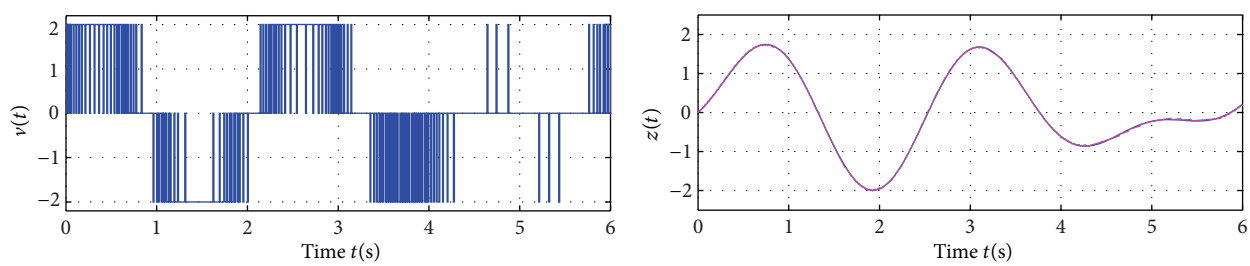

(a) (b)

FIGURE 5: Time responses of Σ_Q with (B.2) for $h = 0.01$.

See Appendix B. The continuous-time quantizer Q_d^{op} and its performance are parameterized by the free parameter $f \in \mathbb{R}_+$. For the simulation, we consider a two-step design for Q_d^{op}; we first set f and second insert the operator HS in the obtained Q_d^{op}. Also, the achievable performance of $J_{HS}(Q_d^{op})$ is calculated by **(Aop)**.

For the comparison, we set the switching speed $h = 0.01$ [s] and the quantization interval $d = 2$. First, we set $f = 50$ and then obtain Q_d^{op} with $\gamma_c = 0.102$. Also, $\gamma(h) = 0.219$ for $J_{HS}(Q_d^{op})$ is obtained from **(Aop)**. Second, we solve the problem **(Sop)** and obtain $\gamma(h) = 0.219$ and the matrix $C_Q = [-19.26 \quad -22.72]$. In this case, both quantizers can approximate well. Figures 4 and 5 illustrate the simulation results of the time responses of Σ_Q with the proposed quantizer and the quantizers Q_d^{op} in (B.2). The initial state $x_0 = [0 \quad 0]^T$ and the input $u(t) = \sin \pi t + \cos 0.7\pi t$ are given. In Figures 4 and 5, the thin lines and the thick lines are for the conventional system in Figure 1(b) and the system Σ_Q in Figure 1(a), respectively. We see that the controlled outputs of the discrete-valued input systems with the dynamic quantizers approximate those of the usual systems even if the quantized outputs are applied. Also, the two controlled outputs approximated by both quantizers are exactly the same.

Next, we consider the case $h = 0.1$. In this case, the two controlled outputs approximated by the two quantizers differ. **(Aop)** for Q_d^{op} is infeasible. From **(Sop)**, on the other hand, we obtain $\gamma(h) = 0.949$ and the matrix $C_Q = [-1.1321 \quad -3.097]$. Figures 6 and 7 illustrate the simulation results on the time responses of Σ_Q with (B.2) and the proposed quantizer in the same fashion. We see that $z(t)$ of the usual plant P is approximated by $z(t)$ of the system Σ_Q with the proposed quantizer, while $z(t)$ of the system Σ_Q with (B.2) diverges. From this example, we see that the proposed method can address the spatial resolution and the temporal resolution issues, simultaneously. Also, Theorem 10 verifies whether the quantizer Q_d^{op} is applicable to the given switching speed setting.

Remark 13. In the above numerical experiments, the proposed quantizer is designed and the quantizer Q_d^{op} is analyzed for $u = HSF(\sin \pi t + \cos 0.7\pi t)$, while the time responses of the quantizers are simulated for $u = \sin \pi t + \cos 0.7\pi t$. That is, this is the conservativeness caused by the signal assumption (15). However, we see that the above results verify the effectiveness of the proposed method even if the signal conservativeness exists.

Here, we focus on the eigenvalues of $\mathscr{A}$ for the system Σ with Q_d^{op}. The eigenvalues for $f = 50$ and $h = 0.1$ are $\{0.741, 0.819, 0.550, -4.21\}$ and then $\mathscr{A}$ is unstable in the discrete-time domain. From Theorem 10, **(Aop)** is infeasible if $\rho(\mathscr{A})$ is bigger than 1 (in other words, $\mathscr{A}$ is unstable). $\{0.741, 0.819\}$ are the eigenvalues of e^{Ah}. That is, $e^{A_Q h} + \int_0^h e^{A_Q \tau} d\tau B_Q C_Q (=: A_Q(h))$ for Q_d^{op} is unstable. Then, we consider the case in which $f = 3$ and $h = 0.1$ ($\gamma_c = 0.707$) such that $A_Q(h)$ is stable. The corresponding eigenvalues are $\{0.637, 0.354\}$. In this case, $\gamma(h) = 1.085$ for $J_{HS}(Q_d^{op})$ is obtained from **(Aop)**.

From the above results, the existing continuous-quantizer in [15, 16] may be suitable for a two-step design such that $A_Q(h)$ is stable via the parameter f. In terms of the upper

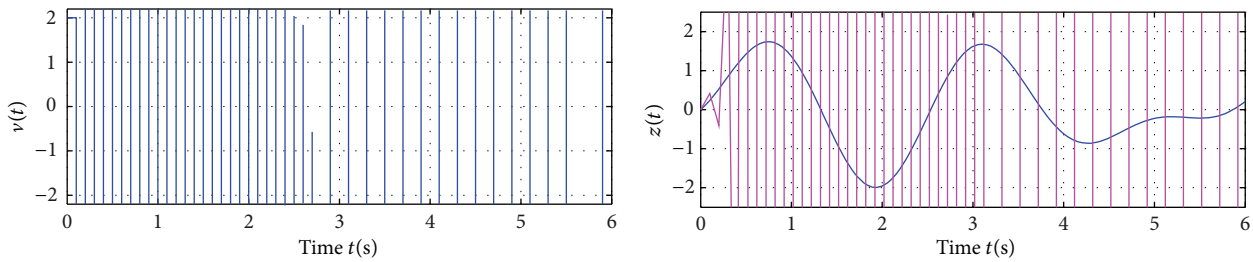

(a) (b)

FIGURE 6: Time responses of Σ_Q with (B.2) for $h = 0.1$.

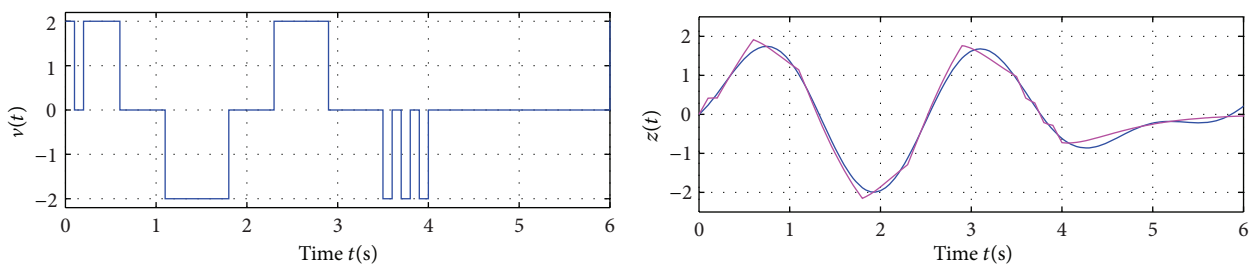

(a) (b)

FIGURE 7: Time responses of Σ_Q with the proposed quantizer for $h = 0.1$.

bound of cost function (B.3), first, let us consider the problem **(P-1)**: maximize f for Q_d^{op} such that

$$\exists X^T = X > 0 \quad \text{s.t. } A_Q(h)^T X A_Q(h) - X < 0, \tag{46}$$

where the parameters (A_Q, B_Q, C_Q) of $A_Q(h)$ are given by (B.2). This problem is LMI for the line search of f. For $h = 0.1$, its solution is $f = 18.9$ ($\gamma_c = 0.173$). However, $\gamma(h) = 113.148$ for $J_{HS}(Q_d^{op})$ is obtained from **(Aop)**. By using Theorem 10, next, let us consider the problem **(P-2)**:

$$\begin{gathered}\min_{\mathcal{Q}=\mathcal{Q}^T>0, S=s_\theta I_n>0, 1/2h-(\rho(\mathcal{A})^2)/2h\geq\alpha_h\geq 0, f>0, \gamma>0} \gamma^2 \\ \text{s.t. } (31) \text{ and } (32),\end{gathered} \tag{47}$$

where the parameters (A_Q, B_Q, C_Q) of Ψ_h and Γ_h are given by (B.2). This problem is LMI for the plane search of f and α_h. For $h = 0.1$, its solution is $f = 5.715$ ($\gamma_c = 0.397$) and then $\gamma(h) = 0.949$ for $J_{HS}(Q_d^{op})$ is obtained. This performance is about the same as that of the proposed quantizer. Therefore, we see that Theorem 10 is also helpful for the two-step design of the existing continuous-time quantizer [15, 16] even if the tractable optimization method instead of the plane search remains an issue for future work. Such a method correlates the parameter f with the switching speed h, so its insight is expected not only to result in a new two-step design but also to clarify the relationship between the discrete-time and continuous-time dynamic quantizers. Of course, important future topics also include considering the quantized feedback control system with unstable plants and generalizing the exogenous signal for the evaluation of the cost function.

5. Conclusion

Focusing on the broadbandization and the robustness of the networked control systems, this paper has dealt with the continuous-time quantized control. We have proposed numerical optimization methods analyzing and synthesizing the continuous-time dynamic quantizer on the basis of the invariant set analysis and the sampled-data control technique. The contributions of the proposed method can be summarized as follows.

(i) Both the temporal and spatial resolution constraints can be simultaneously considered, whereas Ishikawa et al. [20] considered the two constraints step-by-step and we [15, 16] previously ignored the temporal constraint in synthesis. As a result, the proposed method is applicable to both the slow and fast switching cases.

(ii) The maximum output difference for each sampling interval is proven to be evaluated numerically via the matrix uncertainty approach, while the existing results [11–14] evaluate that only for each sampling instance.

(iii) The analysis and synthesis conditions are given in terms of BMIs. However, the quantizer analysis and synthesis problems are reduced to tractable optimization problems.

(iv) The new insight is presented for the existing continuous-time quantizer design [15, 16].

Also, this paper has clarified the following areas for future work.

(i) Because of the feedforward structure, the plant is restricted to be stable. To address unstable systems, we

need to propose design methods for feedback control systems.

(ii) The sensors and actuators are distributed in the networked control system [31], so it is necessary to design multiple (decentralized) quantizers rather than a centralized quantizer similar to the existing ones [14, 16].

(iii) The class of exogenous signals evaluating the cost function is restricted. To avoid this conservativeness, it is necessary to propose the equivalent discrete-time expression instead of (11) using adjoint operator similar to sampled-data control [25, 32].

(iv) For networked control applications, it is important to consider the time-varying sampling period, time delay, packet loss, and so on similar to [6–10]. For example, the works [6, 8] using the LMI technique address time-varying sampling period and time delay, so it is expected that our method using the LMI technique also extends to such problems.

Appendix

A. Proof

The proof of Lemma 4 is as follows.

Proof. $z(kh+\theta)$ for $k = 0, 1, 2, \ldots, \theta \in [0, h)$ (which is the behavior of $z(t)$ over the kth sampling interval) is given by the discretized system of P:

$$\begin{aligned} x[k+1] &= e^{Ah}x[k] + \int_0^h e^{A(h-\tau)}Bv(kh+\tau)\,\mathrm{d}\tau \\ z(kh+\theta) &= Ce^{A\theta}x[k] + C\int_0^\theta e^{A(\theta-\tau)}Bv(kh+\tau)\,\mathrm{d}\tau, \end{aligned} \tag{A.1}$$

where $x[k] = x(kh)$. $v(t)$ is given by (9) and $v_Q[k]$ is given by the discretized system of Q:

$$\begin{aligned} x_Q[k+1] &= \left(e^{A_Q h} + \int_0^h e^{A_Q\tau}\mathrm{d}\tau B_Q C_Q\right)x_Q[k] + \int_0^h e^{A_Q\tau}\mathrm{d}\tau B_Q e[k] \\ &\quad + \int_0^h e^{A_Q(h-\tau)}B_Q\tilde{u}(kh+\tau)\,\mathrm{d}\tau, \\ v_Q[k] &= C_Q x_Q[k], \end{aligned} \tag{A.2}$$

where $x_Q[k] = x_Q(kh)$. This is because e_Q is given by

$$e_Q = \hat{v}_Q + e + \hat{u} - u, \qquad \hat{v}_Q = HSv_Q, \qquad \hat{u} = HSu. \tag{A.3}$$

Then, $z(kh+\theta, x_0, Q_d(u))$ for $k = 0, 1, 2, \ldots, \theta \in [0, h)$ is expressed by the discretized system of Σ_Q:

$$\Sigma_Q^d : \begin{cases} \begin{bmatrix} x[k+1] \\ x_Q[k+1] \end{bmatrix} \\ \quad = \mathscr{A}\begin{bmatrix} x[k] \\ x_Q[k] \end{bmatrix} + \mathscr{B}e[k] \\ \quad + \begin{bmatrix} \int_0^h e^{A(h-\tau)}Bu[k]\,\mathrm{d}\tau \\ \int_0^h e^{A_Q(h-\tau)}B_Q\tilde{u}(kh+\tau)\,\mathrm{d}\tau \end{bmatrix}. \\ z(kh+\theta) \\ \quad = \mathscr{C}(\theta)\begin{bmatrix} x[k] \\ x_Q[k] \end{bmatrix} + \mathscr{D}(\theta)e[k] \\ \quad + C\int_0^\theta e^{A(h-\tau)}Bu[k]\,\mathrm{d}\tau \end{cases} \tag{A.4}$$

Also, $z^*(kh+\theta, x_0, u)$ for $k = 0, 1, 2, \ldots, \theta \in [0, h)$ without the quantizer is given by

$$P_d^* : \begin{cases} \hat{x}[k+1] \\ \quad = e^{Ah}\hat{x}[k] + \int_0^h e^{A(h-\tau)}Bu(kh+\tau)\,\mathrm{d}\tau \\ z^*(kh+\theta) \\ \quad = Ce^{A\theta}\hat{x}[k] + C\int_0^\theta e^{A(h-\tau)}u(kh+\tau)\,\mathrm{d}\tau, \end{cases} \tag{A.5}$$

where $\hat{x}(0) = x_0$ and $\hat{x}[k] = \hat{x}(kh)$. From Σ_Q^d and P_d^*, we obtain the system Σ in (11). □

For the proof of Theorem 10, we use the S-procedure [23, 28, 29].

Lemma A.1. *For the real matrices L, M, and N of appropriate size, the inequality*

$$L + M\Delta N + N^T\Delta^T M^T \geq 0 \tag{A.6}$$

holds for any matrix Δ such that $\sigma_{\max}(\Delta) \leq \delta$ if and only if there exists a matrix $S = S^T > 0$ such that

$$\begin{bmatrix} L - \delta MSM^T & \sqrt{\delta}N^T \\ \sqrt{\delta}N & S \end{bmatrix} \geq 0, \quad S\Delta = \Delta S. \tag{A.7}$$

Then, the proof of Theorem 10 is as follows.

Proof. We use Lemmas 9 and A.1 with

$$\begin{aligned} L &= \begin{bmatrix} \mathscr{P} & \widehat{\mathscr{C}}^T \\ \widehat{\mathscr{C}} & \gamma^2 I_q \end{bmatrix}, \qquad M = \begin{bmatrix} 0 \\ C \end{bmatrix}, \\ N &= \begin{bmatrix} \widehat{\mathscr{D}} & 0 \end{bmatrix}, \qquad \Delta = \Omega(\theta). \end{aligned} \tag{A.8}$$

In this case, for the inequalities (25), we obtain their sufficient conditions as follows:

$$\gamma_1 \le \gamma \quad \text{s.t.} \begin{cases} \begin{bmatrix} \mathscr{P} & \widehat{\mathscr{C}}^T & \sqrt{\delta(h)}\widehat{\mathscr{D}}^T \\ \widehat{\mathscr{C}} & \gamma^2 I_q - \delta(h) CSC^T & 0 \\ \sqrt{\delta(h)}\widehat{\mathscr{D}} & 0 & S \end{bmatrix} \ge 0, \\ S\Omega(\theta) = \Omega(\theta) S, \qquad \forall \theta \in [0, h) \end{cases}$$

$$\begin{aligned} \gamma_2 &\le \sigma_{\max}(C)\,\delta(h) \quad \text{s.t.} \quad \Omega(\theta)^T C^T C \Omega(\theta) \\ &\le \sigma_{\max}(C)^2 \delta(h)^2 I_n, \quad \forall \theta \in [0, h). \end{aligned} \tag{A.9}$$

Then, the upper bound of $J_{HS}(Q_d)$ is given by (30). By substituting $\mathscr{A} = I + h\Phi_h$ and $\mathscr{B} = h\Gamma_h$ into (20), we obtain

$$\begin{aligned} &\begin{bmatrix} \mathscr{A}^T \mathscr{P} \mathscr{A} - (1-\alpha)\mathscr{P} & \mathscr{A}^T \mathscr{P} \mathscr{B} \\ \mathscr{B}^T \mathscr{P} \mathscr{A} & \mathscr{B}^T \mathscr{P} \mathscr{B} - \alpha I_m \end{bmatrix} \\ &= \begin{bmatrix} (I + h\Phi_h)^T \mathscr{P} (I + h\Phi_h) - (1-\alpha)\mathscr{P} & h(I + h\Phi_h)^T \mathscr{P} \Gamma_h \\ h\Gamma_h^T \mathscr{P} (I + h\Phi_h) & h^2 \Gamma_h^T \mathscr{P} \Gamma_h - \alpha I_m \end{bmatrix} \\ &= h \begin{bmatrix} \Phi_h^T \mathscr{P} + \mathscr{P}\Phi_h + \alpha/h\mathscr{P} & \mathscr{P}\Gamma_h \\ \Gamma_h^T \mathscr{P} & -\alpha/hI_m \end{bmatrix} \\ &\quad + h \begin{bmatrix} \sqrt{h}\Phi_h^T \\ \sqrt{h}\Gamma_h^T \end{bmatrix} \mathscr{P} \begin{bmatrix} \sqrt{h}\Phi_h & \sqrt{h}\Gamma_h \end{bmatrix} \le 0. \end{aligned} \tag{A.10}$$

By Schur complement [29], (A.10) is equivalent to (31) where $\mathscr{Q} = \mathscr{P}^{-1}$ and $\alpha_h = \alpha/2h$. Also, (A.9) is equivalent to (32) where $\mathscr{Q} = \mathscr{P}^{-1}$. □

B. Continuous-Time Dynamic Quantizer [15, 16]

For the system $\widehat{\Sigma}$ in (34) without the operator HS, we consider the following non-convex optimization ($\mathbf{OP}'$):

$$\begin{aligned} &\min_{\mathscr{P}>0, \mu(\widehat{\mathscr{A}}) \ge \alpha \ge 0, A_Q, B_Q, C_Q, \gamma_c > 0} \quad \gamma_c \\ &\text{s.t.} \quad \begin{bmatrix} \widehat{\mathscr{A}}^T \mathscr{P} + \mathscr{P}\widehat{\mathscr{A}} + 2\alpha\mathscr{P} & \mathscr{P}\widehat{\mathscr{B}} \\ \widehat{\mathscr{B}}^T \mathscr{P} & -2\alpha I_m \end{bmatrix} \le 0, \\ &\qquad \begin{bmatrix} \mathscr{P} & \widehat{\mathscr{C}}^T \\ \widehat{\mathscr{C}} & \gamma_c^2 I_q \end{bmatrix} \ge 0. \end{aligned} \tag{B.1}$$

The dynamic quantizer without the operator HS is obtained from ($\mathbf{OP}'$) and $J(Q_d) \le \gamma_c$ is achieved. Also, an optimal form of the continuous-time quantizer [15, 16] is given by

$$Q_d^{op} : \begin{cases} \dot{x}_Q = Ax_Q + B(v - u) \\ v = q\left(-(CB)^{-1} C (A + fI) x_Q + u\right), \end{cases} \tag{B.2}$$

where its achievable upperbound of $J(Q_d^{op})$ is characterized by

$$\begin{aligned} \inf \gamma_c &= \frac{d\sqrt{m}}{4\sqrt{|g|(f - |g|)}} \sigma_{\max}(CB), \\ g &= \max\left\{\nu(A), \nu\left(A - B(CB)^{-1} C (A + fI)\right)\right\}, \end{aligned} \tag{B.3}$$

where $\nu(A) := \max\{\mathrm{Re}(\lambda) : \lambda \in \mathrm{eig}(A)\}$. The continuous-time quantizer Q_d^{op} and its performance are parameterized by the free parameter $f \in \mathbb{R}_+$. Note that the larger values of f not only provide the better approximation performance, but also switch the outputs v, more quickly. In other words, the quantizer from ($\mathbf{OP}'$) results in the switching that is too fast and is sometimes not applicable to the slow switching case.

Acknowledgments

The authors would like to thank the reviewers for their valuable comments. This work was partly supported by Grant-in-Aid for Young Scientists (B) no. 24760332 from the Ministry of Education, Culture, Sports, Science and Technology of Japan.

References

[1] W. S. Wong and R. W. Brockett, "Systems with finite communication bandwidth constraints. II: stabilization with limited information feedback," *IEEE Transactions on Automatic Control*, vol. 44, no. 5, pp. 1049–1053, 1999.

[2] N. Elia and S. K. Mitter, "Stabilization of linear systems with limited information," *IEEE Transactions on Automatic Control*, vol. 46, no. 9, pp. 1384–1400, 2001.

[3] M. Fu and L. Xie, "The sector bound approach to quantized feedback control," *IEEE Transactions on Automatic Control*, vol. 50, no. 11, pp. 1698–1711, 2005.

[4] J. Baillieul, "Special issue on networked control systems," *IEEE Transactions on Automatic Control*, vol. 49, no. 9, pp. 1421–1423, 2004.

[5] P. Antsaklis and J. Baillieul, "Special issue on technology of networked control systems," *Proceedings of the IEEE*, vol. 95, no. 1, pp. 5–8, 2007.

[6] D. Yue, E. Tian, Z. Wang, and J. Lam, "Stabilization of systems with probabilistic interval input delays and its applications to networked control systems," *IEEE Transactions on Systems, Man, and Cybernetics A*, vol. 39, no. 4, pp. 939–945, 2009.

[7] W. P. M. H. Heemels, A. R. Teel, N. van de Wouw, and D. Nešić, "Networked control systems with communication constraints: tradeoffs between transmission intervals, delays and performance," *IEEE Transactions on Automatic Control*, vol. 55, no. 8, pp. 1781–1796, 2010.

[8] B. Shen, Z. Wang, and X. Liu, "Sampled-data synchronization control of complex dynamical networks with stochastic sampling," *IEEE Transactions on Automatic Control*, vol. 57, no. 10, pp. 2644–2650, 2012.

[9] W. P. M. H. Heemels, M. C. F. Donkers, and A. R. Teel, "Periodic event-triggered control for linear systems," *IEEE Transactions on Automatic Control*, vol. 58, no. 4, pp. 847–861, 2013.

[10] K. Okano and H. Ishii, "Networked control of uncertain systems over data rate limited and lossy channels," *IEICE Transactions on Fundamentals of Electronics, Communications and Computer Sciences*, vol. E96-A, no. 5, pp. 853–860, 2013.

[11] S. Azuma and T. Sugie, "Optimal dynamic quantizers for discrete-valued input control," *Automatica*, vol. 44, no. 2, pp. 396–406, 2008.

[12] S. Azuma and T. Sugie, "Synthesis of optimal dynamic quantizers for discrete-valued input control," *IEEE Transactions on Automatic Control*, vol. 53, no. 9, pp. 2064–2075, 2008.

[13] K. Sawada and S. Shin, "Synthesis of dynamic quantizers for quantized feedback systems within invariant set analysis framework," in *Proceedings of the American Control Conference (ACC '11)*, pp. 1662–1667, July 2011.

[14] Y. Minami, S. Azuma, and T. Sugie, "Optimal decentralized sigma-delta modulators for quantized feedback control," *IEICE Nonlinear Theory and Its Applications*, vol. 3, no. 3, pp. 386–404, 2012.

[15] K. Sawada and S. Shin, "Synthesis of continuous-time dynamic quantizer for quantized feedback systems," in *Proceedings of the 4th IFAC Conference on Analysis and Design of Hybrid Systems (ADHS '12)*, pp. 2488–2493, 2012.

[16] K. Sawada and S. Shin, "On numerical optimization design of continuous-time feedback type quantizer for networked control systems," in *Proceedings of the 8th IEEE International Conference on Automation Science and Engineering (CASE '12)*, pp. 1140–1145, 2012.

[17] K. Reddy and S. Pavan, "Fundamental limitations of continuous-time delta-sigma modulators due to clock jitter," *IEEE Transactions on Circuits and Systems I*, vol. 54, no. 10, pp. 2184–2194, 2007.

[18] K. Matsukawa, Y. Mitani, M. Takayama, K. Obata, S. Dosho, and A. Matsuzawa, "A fifth-order continuous-time delta-sigma modulator with single-opamp resonator," *IEEE Journal of Solid-State Circuits*, vol. 45, no. 4, pp. 697–706, 2010.

[19] M. Koike and Y. Chida, "Vibration control design considering quantization error for an on-off control system including input time-delay," in *Proceedings of the 50th Annual Conference on Society of Instrument and Control Engineers (SICE '11)*, pp. 760–765, September 2011.

[20] M. Ishikawa, I. Maruta, and T. Sugie, "Practical controller design for discrete-valued input systems using feedback modulators," in *Proceedings of the European Control Conference (ECC '07)*, Kos, Greece, July 2007.

[21] R. Sanchez-Peña and M. Sznaier, *Robust Systems Theory and Applications*, John Wiley & Sons, 1998.

[22] H. Shingin and Y. Ohta, "Optimal invariant sets for discrete-time systems: approximation of reachable sets for bounded inputs," in *Proceedings of the 10th IFAC/IFORS/IMACS/IFIP Symposium on Large Scale Systems, Theory and Applications (LSS '04)*, pp. 401–406, 2004.

[23] Y. Oishi and H. Fujioka, "Stability analysis of aperiodic sampled-data control systems: an improved approach using matrix uncertainty," in *Proceedings of the 19th International Symposium on Mathematical Theory of Networks and Systems (MTNS '10)*, pp. 1147–1152, July 2010.

[24] Y. Oishi and H. Fujioka, "Stability and stabilization of aperiodic sampled-data control systems using robust linear matrix inequalities," *Automatica*, vol. 46, no. 8, pp. 1327–1333, 2010.

[25] T. Chen and B. Francis, *Optimal Sampled-Data Control Systems*, Springer, 1995.

[26] G. H. Golub and C. F. van Loan, *Matrix Computations*, Johns Hopkins Studies in Mathematical Sciences, Johns Hopkins University Press, 3rd edition, 1996.

[27] H. Fujioka, "Command shaping for sampled-data servo systems with constraints," *Transactions of the Institute of Systems, Control and Information Engineers*, vol. 19, no. 7, pp. 284–289, 2006 (Japanese).

[28] M. Fu and N. E. Barabanov, "Improved upper bounds for the mixed structured singular value," *IEEE Transactions on Automatic Control*, vol. 42, no. 10, pp. 1447–1452, 1997.

[29] S. Boyd, L. E. Ghaoui, E. Feron, and V. Balakrishnan, *Linear Matrix Inequalities in System and Control Theory*, vol. 15 of *Studies in Applied Mathematics*, SIAM, 1994.

[30] I. Masubuchi, A. Ohara, and N. Suda, "LMI-based controller synthesis: a unified formulation and solution," *International Journal of Robust and Nonlinear Control*, vol. 8, no. 8, pp. 669–686, 1998.

[31] J. A. Stankovic, "When sensor and actuator networks cover the world," *ETRI Journal*, vol. 30, no. 5, pp. 627–633, 2008.

[32] Y. Hayakawa, S. Hara, and Y. Yamamoto, "H_∞ type problem for sampled-data control systems—a solution via minimum energy characterization," *IEEE Transactions on Automatic Control*, vol. 39, no. 11, pp. 2278–2284, 1994.